Catalysis Letters Vol. 110, Nos. 3–4, September 2006 (© 2006)
DOI: 10.1007/s10562-006-0119-6

Effect of the support on the mechanism of partial oxidation of methane on platinum catalysts

Fabio B. Passos,[a,*] Elaine R. Oliveira,[a] Lisiane V. Mattos,[b] and Fabio B. Noronhe[b]

[a]*Universidade Federal Fluminense, Rua Passo da Pátria, CEP 24210-240 156 Niterói – RJ, Brazil*
[b]*Instituto Nacional de Tecnologia, Av. Venezuela, CEP 20081-312 82 Rio de Janeiro – RJ, Brazil*

Received 3 March 2006; accepted 6 May 2006

The partial oxidation of methane was studied on Pt/Al_2O_3, Pt/ZrO_2, Pt/CeO_2 and Pt/Y_2O_3 catalysts. For Pt/Al_2O_3, Pt/ZrO_2 and Pt/CeO_2, temperature programmed surface reaction (TPSR) studies showed partial oxidation of methane comprehends two steps: combustion of methane followed by CO_2, and steam reforming of unreacted methane, while for Pt/Y_2O_3 a direct mechanism was observed. Oxygen Storage Capacity (OSC) evaluated the reducibility and oxygen transfer capacity of the catalysts. Pt/CeO_2 catalyst showed the highest stability on partial oxidation. The results were explained by the higher reducibility and oxygen storage/release capacity which allowed a continuous removal of carbonaceous deposits from the active sites, favoring the stability of the catalyst, For Pt/Al_2O_3 and Pt/ZrO_2 catalysts the increase of carbon deposits around or near the metal particle inhibits the CO_2 dissociation on CO_2 reforming of methane. Pt/Y_2O_3 was active and stable for partial oxidation of methane, and its behavior was explained by a change in the reaction mechanism.

KEY WORDS: Methane; Natural gas; Partial oxidation; Pt/CeO_2; Pt/Y_2O_3.

1. Introduction

The main uses of the natural gas are related to its combustion for home and industrial heating purposes, and for the electrical energy generation market. Only a small fraction of the natural gas is employed as a feedstock for the chemical industry, despite of its relatively high abundance [1]. The development of competitive technologies for the conversion of natural gas to liquid hydrocarbons (GTL) would be a good opportunity to better employ the natural gas, with the production of more efficient and environmental friendly fuels. The classical GTL route comprehends the synthesis gas (H^2 and CO) production, followed by the formation of liquid hydrocarbons through the Fischer-Tropsch synthesis. The leading industrial process for synthesis gas generation is the catalytic steam reforming of methane. This reaction is highly endothermic, requiring elevated temperatures and pressures in order to favor high conversions at chemical equilibrium. Consequently, these conditions lead to high catalyst deactivation rates and to high plant operation costs. This way, the economical viability of GTL technology strongly depends on the development of more efficient routes for synthesis gas generation [2].

Partial oxidation of methane is an interesting alternative for synthesis gas generation. The reaction is mildly exothermic and produces a synthesis gas with a H_2/CO ratio equal to 2, which is suitable for the subsequent use in the Fischer-Tropsch synthesis [3–5]. A two-step mechanism has been proposed for the partial oxidation of methane. The first step is the total combustion of part of the methane producing carbon dioxide and steam. In the second step, synthesis gas is generated through methane reforming with steam and/or carbon dioxide [4]. On the other hand, a direct mechanism was reported for Ru/TiO_2 [6], $Ni/CaO{\cdot}Al_2O_3$ [7] and ytria-zirconia [8] catalysts.

One of the main drawbacks for methane conversion is the deactivation due to coke formation, thus there is a great interest on designing catalysts that minimize the deleterious effect of coke. The presence of oxygen vacancies in the support proved to be instrumental in keeping metal particles free from coke deposition [9, 10]. In this work, the use of platinum catalysts supported on different oxides (Al_2O_3, ZrO_2, CeO_2 and Y_2O_3) was investigated in the partial oxidation of methane. The effect of the oxygen storage capacity on the stability of the catalysts is reported as well as the effect of the support on the controlling mechanism of the reaction.

2. Experimental

2.1. Catalyst preparation

Al_2O_3, CeO_2, ZrO_2 and Y_2O_3 were prepared by calcination of γ-Al_2O_3, $(NH_4)_2Ce(NO_3)_6$, $Zr(OH)_4$ and $Y(NO_3)_3$, respectively at 800 °C for 1 h. Other ceria

*To whom correspondence should be addressed.
E-mail: fbpassos@vm.uff.brE-mail: fabiobel@int.gov.br

sample (CeO_2 ppt) was prepared by a precipitation method as described by Hori et al. [11]. The catalysts were prepared by an incipient wetness technique using an $H_2PtCl_6{\cdot}6H_2O$ aqueous solution and were dried at 120 °C. After impregnation, the samples were calcined under air (50 cm^3/min) at 400 °C for 2 h. All samples contained 1.5 wt.% of platinum.

2.2. Surface area measurements

Nitrogen adsorption isotherms on the several catalysts were obtained at 77 K using a Micromeritics ASAP 2010 equipment. The surface area was calculated using the BET method.

2.3. Temperature programmed reduction

Temperature programmed reduction experiments were performed in a quartz microreactor coupled to a quadrupole mass spectrometer (Balzers, Omnistar). The samples (300 mg) were dehydrated at 150 °C for 30 min in a He flow prior to reduction. After cooling to room temperature, a mixture of 5% H_2 in Ar flowed through the sample at 30 cm^3/min, and the temperature was raised at a heating rate of 10 K/min upto 1000 °C.

2.4. Oxygen storage capacity (OSC)

Oxygen storage capacity (OSC) measurements were carried out in a similar apparatus used for TPR experiments. Prior to OSC analysis, the samples were reduced under H_2 at 500 °C for 1 h and heated to 800 °C in flowing He. Then, the samples were cooled to 450 °C and remained at this temperature during the analysis. The mass spectrometer was used to measure the composition of the reactor effluent as a function of time while a 5% O_2/He mixture was passed through the catalyst. The reactor was purged with He and the dead volume was obtained by switching the gas back to the 5%O_2/He mixture. Oxygen consumption was calculated from the curve corresponding to $m/e = 32$ taking into account a previous calibration of the mass spectrometer.

2.5. Temperature programmed surface reaction (TPSR)

Temperature programmed surface reaction (TPSR) experiments were performed in the same apparatus used for TPR measurements. After the activation protocol, the sample (300 mg) was purged in He at 800 °C for 30 min, and cooled to room temperature. Then the sample was submitted to a flow of CH_4/O_2/He (2:1:27) at 30 cm^3/min while the temperature was raised up to 800 °C at heating rate of 20 °C /min.

2.6. Cyclohexane dehydrogenation

Cyclohexane dehydrogenation was used as a structure-insensitive reaction to evaluate the number of exposed Pt atoms of the samples [12]. Since H_2 and CO adsorption occurs over CeO_2 support, platinum dispersion could not be determined from chemisorption of both gases [13]. Then, in order to estimate the dispersion of Pt/ZrO_2, Pt/CeO_2, Pt/CeO_2 ppt and Pt/Y_2O_3 catalysts, a correlation between the rate of cyclohexane dehydrogenation and platinum dispersion measured by hydrogen chemisorption on Pt/Al_2O_3 catalysts was employed. This reaction was performed under atmospheric pressure in a continuous flow micro-reactor. The pretreatment of the samples (10 mg) consisted of drying at 150 °C under 30 cm^3/min of N_2 flow for 30 min, followed by reduction at 500 °C under a H_2 flow (30 cm^3/min). The reactant mixture was obtained by bubbling hydrogen through a saturator containing cyclohexane at 12 °C ($H_2/C_6H_{12} = 13.6$). The total flow rate was 100 cm^3/min and temperature was 270 °C. At these conditions, the conversion was kept below 10%. The effluent gas phase was analyzed by an on-line gas chromatograph (HT 5890) equipped with a flame ionization detector and a HPINNOWax capillary column.

2.7. Partial oxidation of methane

Partial oxidation of methane was performed in a quartz reactor (13 mm i.d.) at atmospheric pressure. Prior to reaction, the catalyst was reduced under H_2 at 500 °C for 1 h and then heated to 800 °C under N_2. The reaction was carried out at 800 °C and WHSV = 520 h^{-1} over all catalysts. A reactant mixture with CH_4:O_2 ratio of 2:1 and a flow rate of 100 cm^3/min was used. In order to avoid temperature gradients, catalyst samples (10 mg) were diluted with inert SiC (18 mg) and the bed height being around 3 mm. The transfer lines were kept at 140 °C to avoid condensation. The exit gases were analyzed using a gas chromatograph (Agilent 6890) equipped with a thermal conductivity detector and a CP-carboplot column (Chrompack).

3. Results

3.1. Oxygen storage capacity and surface area measurements

Oxygen storage capacity results and BET surface areas for all the catalysts are presented in table 1. Pt/Al_2O_3 and Pt/Y_2O_3 catalysts did not present any O_2 uptake, while for Pt/ZrO_2 and Pt/CeO_2 ppt these values

Table 1
Oxygen storage capacity of Pt catalysts

Catalyst	O_2 uptake (μmol/g_{cat})	Surface area (m^2/g)
Pt/Al_2O_3	0	180
Pt/ZrO_2	9	20
Pt/CeO_2	194	14
Pt/Y_2O_3	0	17
Pt/CeO_2 ppt	18	9

were rather low. Pt/CeO_2 was the only catalyst that showed a considerable oxygen storage capacity. The BET surface areas of the catalysts presented typical values for the several supports used. Pt/Al_2O_3 showed the higher surface area (180 m^2/g) while for the other catalysts the surface areas were similar ranging from 9 to 20 m^2/g.

3.2. Temperature programmed reduction

Figure 1 presents the temperature programmed reduction profiles for the supports used in this study. Al_2O_3 did not exhibit any reduction under the tested conditions. The TPR profile for CeO_2 presented two maxima at 550 °C and 960 °C, respectively. Based on the H_2 consumption of the TPR experiments, the degree of reduction of CeO_2 was calculated as 30%. The TPR profile of ZrO_2 showed a very small hydrogen uptake around 650 °C, with the amount of hydrogen consumed corresponding to a degree of reduction of about 0.2%. In the case of Y_2O_3, the reduction was also not significant, with a small and broad peak around 500 °C, and with the consumption of H_2 corresponding to a reduction degree around 1%.

The temperature programmed reduction profiles for the platinum supported catalysts are shown in figure 2. Pt/Al_2O_3 showed a main reduction peak at 220 °C and a shoulder around 330 °C. Over the Pt/CeO_2 catalyst, two peaks were observed at 185 °C and 970 °C, respectively. Based on the H_2 consumption during the TPR, the CeO_2 degree of reduction was 30%, showing that the presence of platinum did not increase the amount of reduced CeO_2.

One major peak at 205°C was observed for the Pt/ZrO_2 catalyst with a minor reduction at 370 °C. The degree of reduction of the ZrO_2 was less than 1% for this catalyst. The TPR profile of Pt/Y_2O_3 was quite distinct from the other catalysts. There was the formation of a small peak at 270°C and of a large one at 420°C. The amount of reduced Y_2O_3 in the catalyst was slightly higher than observed for the support (around, 4% degree of reduction).

3.3. TPSR experiments

Figure 3 shows the TPSR profile obtained for Pt/Al_2O_3 catalyst. The Pt/Ce_2O_3, Pt/ZrO_2, and Pt/CeO_2 ppt showed similar profiles. The results obtained for these catalysts are consistent to the partial oxidation of methane proceeding through a two-step mechanism

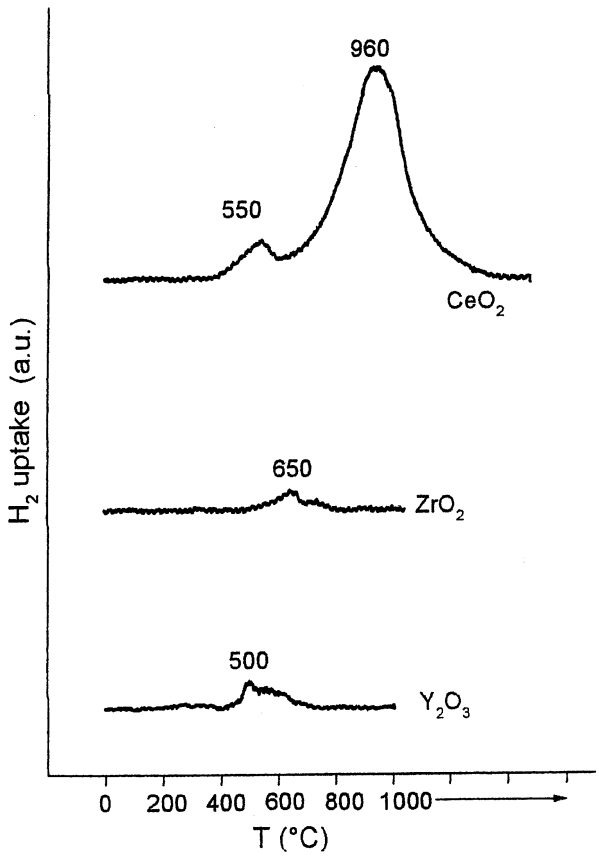

Figure 1. Temperature programmed reduction profiles of the supports.

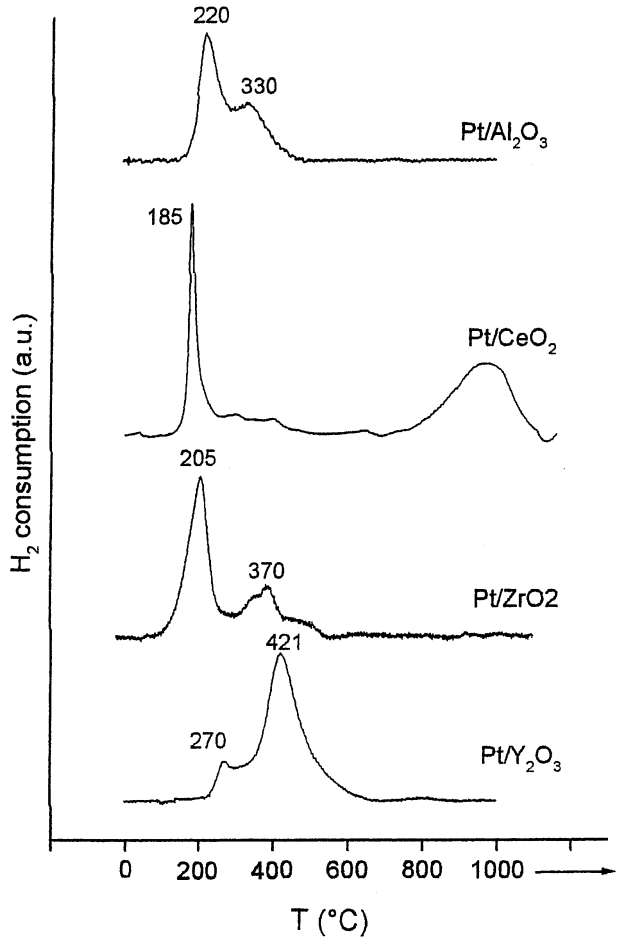

Figure 2. Temperature programmed reduction profiles of Pt catalysts.

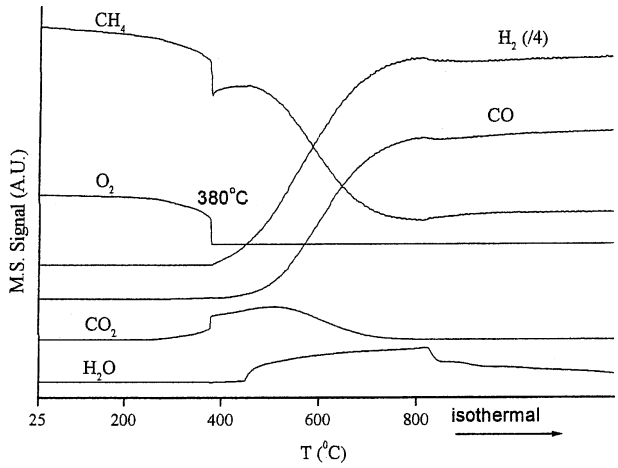

Figure 3. Temperature programmed surface reaction for Pt/Al_2O_3.

(indirect mechanism). For temperatures between 300 °C and 400 °C, Pt/CeO_2, Pt/Al_2O_3, Pt/ZrO_2, and Pt/CeO_2 ppt are active for the total oxidation of methane forming carbon dioxide and water. There is a temperature lag between the formation of CO and the formation of H_2, with H_2 being formed previously probably due to the decomposition of methane. After this step, these catalysts become active for the steam and carbon dioxide reforming generating synthesis gas. The TPSR profile for Pt/Y_2O_3 is displayed in figure 4. The reaction begins at 480 °C, with consumption of CH_4 and O_2 and the formation of H_2, CO, H_2O, and CO_2. There is a consumption of the CO_2 formed at more elevated temperatures pointing to an additional dry reforming reaction. H_2O consumption is not as significant, implying a lower activity for steam reforming. Additionally, there is a quite large difference (ca. 100 °C) between the initial temperature for methane conversion for the several catalysts due to combustion and the initial temperature observed for methane conversion due to a direct formation of CO and H_2 observed for the Pt/Y_2O_3 catalyst.

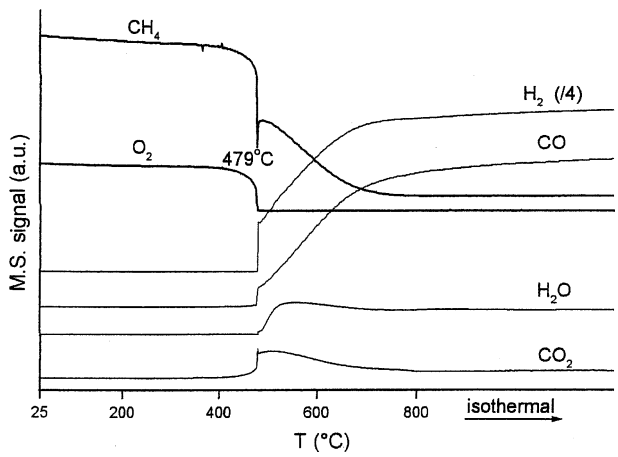

Figure 4. Temperature programmed surface reaction for Pt/Y_2O_3.

Table 2
Dehydrogenation of cyclohexane on Pt catalyts (p = 1 atm, T = 270 °C).

Catalyst	Initial rate ($mol/g_{cat}{\cdot}h$)	Apparent dispersion (%)
Pt/Al_2O_3	0.19	48
Pt/ZrO_2	0.12	29
Pt/CeO_2	0.19	48
Pt/Y_2O_3	0.11	26
Pt/CeO_2 ppt	0.062	15

3.4. Cyclobexane dehydrogenation

The cyclohexane dehydrogenation rates and the platinum dispersion calculated through these rates are listed in table 2. The dispersion increased in the order $Pt/CeO_2ppt < Pt/Y_2O_3 \sim Pt/ZrO_2 < PtCeO_2 \sim Pt/Al_2O_3$.

3.5. Partial oxidation of methane

The results for the partial oxidation of methane on several catalysts are presented in figure 5. Among the catalysts which followed the two-step mechanism, Pt/CeO_2 displayed a higher initial conversion and was active and stable during time on stream (TOS). Moreover, Pt/Al_2O_3 and Pt/ZrO_2 catalysts showed similar initial conversion, but deactivated during time on stream. The Pt/CeO_2 ppt was neither active nor stable in this reaction. On the other hand, Pt/Y_2O_3 catalyst presented a high initial conversion and proved to be as stable as Pt/CeO_2.

Figure 6 shows the change in CO selectivity during time on stream for the several catalysts. In the case of the catalysts which followed the two-step mechanism, and that were not stable, CO selectivity decreased as the methane conversion decreased. In the case of the more stable catalysts, Pt/CeO_2 and Pt/Y_2O_3 presented similar CO selectivities, which were not affected during the time on stream.

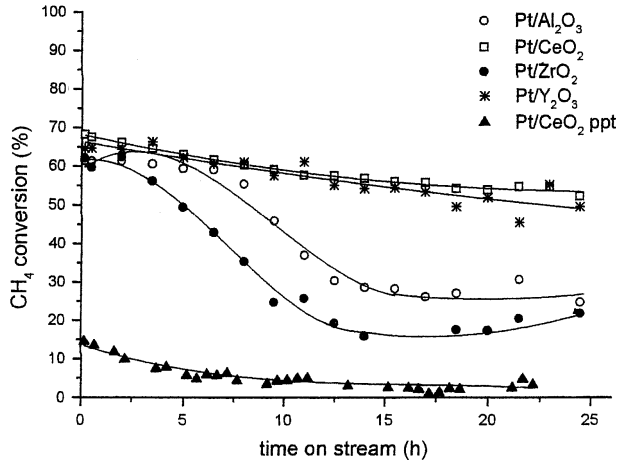

Figure 5. Partial oxidation of methane on Pt catalysts (p = 1 atm, T = 800 °C e CH_4:O_2 2:1, WHSV = 523 h^{-1}).

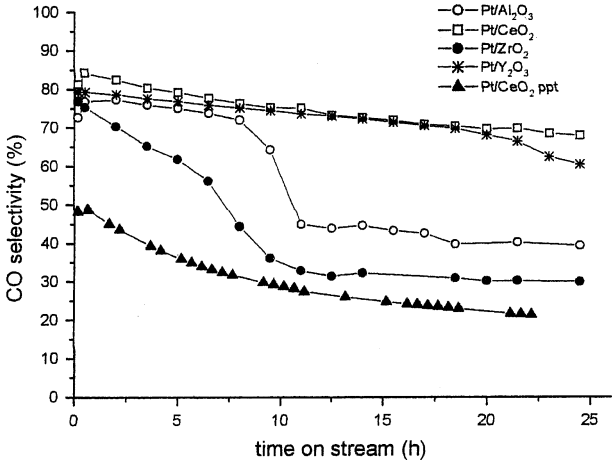

Figure 6. Selectivity to CO in the partial oxidation of methane on Pt catalysts (p = 1 atm, T = 800 °C e CH_4:O_2 = 2:1, WHSV = 523 h^{-1}).

4. Discussion

The TPSR results showed that the nature of the support affected the mechanism of partial oxidation of methane reaction. For the catalysts supported on Al_2O_3, CeO_2 and ZrO_2, the reaction mechanism involved two steps: (i) combustion of methane, producing CO_2 and H_2O and (ii) H_2O and CO_2 reforming of unreacted methane, forming H_2. However, for Pt/Y_2O_3 catalyst, CO, H_2, CO_2 and H_2O were produced through only one step.

Several authors have reported that the mechanism of partial oxidation of methane is strongly affected by the nature of the catalyst. The mechanism of partial oxidation of methane was first studied by Pettre et al. [14] employing a supported Ni catalyst. Based on temperature gradients observed for the catalyst bed, these authors proposed a two-step mechanism with the exothermic combustion of methane yielding CO_2 and steam being followed by the endothermic steam and CO_2 reforming of methane. Dissanayake et al. [15] associated different active species on Ni/Al_2O_3 catalysts to the two-step mechanism, with the previously calcined catalyst bed consisting of three different regions: $NiAl_2O_4$ showing moderate activity for total oxidation of methane, followed by NiO which showed high activity for total combustion, and metallic Ni, which was active for reforming reactions. An indirect mechanism was also observed by Hegarty et al. [16] for Pt/ZrO_2 catalysts, by following changes in the selectivity as a function of the reaction temperature. Similar results indicating a indirect mechanism were observed by Souza and Schmal for Pt/ZrO_2 and $Pt/ZrO_2{\cdot}Al_2O_3$ catalysts [17]. Vermeiren et al. [18] proposed a combination of methane combustion, steam reforming and water–gas shift reaction for Ni-based catalysts.

A direct mechanism involving the pyrolysis of methane ($CH_4 \rightarrow CH_x + (4-x)$ H) followed by the oxidation of carbon species to CO was proposed by Mallens et al. [19] who investigated the partial oxidation mechanism on Pt using pulses of CH_4, O_2 and of CH_4/O_2 mixtures. According to these authors, the methane adsorbs dissociatively on Pt surface sites, forming C and H atoms. The carbon species would be oxidized by PtO_x species, which would also favor the recombination of H atom to form H_2. These authors also proposed that in a parallel reaction CH_4 is directly converted to CO_2 and H_2O by dissolved oxygen which migrates from bulk to surface Pt. A direct mechanism was also proposed by Hu and Ruckenstein [20] for Ni/SiO_2 catalysts, with CH_4 being dissociated before its dissociation. Steghuis et al. [8] have observed different mechanisms depending on the nature of the catalyst tested. In the case of noble metal supported catalysts the reaction occurred via the indirect mechanism, while for Y_2O_3/ZrO_2 there was a two parallel oxidation pathways, i.e. direct partial oxidation ($CH_4 + O_2 \rightarrow CO + H_2 + H_2O$) and full oxidation to CO_2 and H_2O, with both reactions proceeding via a Mars van Krevelen mechanism. In the suggested mechanism, methane is homolitically dissociated and CO, H_2, and H_2O are formed from the decomposition of a formaldehyde precursor, while CO_2 is obtained from decomposition of formed bicarbonate and further oxidation of dioxymethylene. Wheng et al. [21] investigated the mechanism of partial oxidation of methane on Rh/SiO_2, Ru/SiO_2 and Ru/Al_2O_3 catalyts. For Rh/SiO_2 these authors identified CO as a primary product, indicating the direct mechanism for this catalyst. For Ru/SiO_2 and Ru/Al_2O_3 they observed the main route for CO formation is through the reforming reactions. The difference in the mechanisms was explained by different surface oxygen species concentration in these catalytic systems. They suggested that Ru exhibited higher probability to be oxidized than Rh under reaction conditions.

According to Wang et al. [22], the distinction between direct or indirect pathway depends on the concentration of oxygen on metal surface. When the concentration of oxygen is low, CO and H_2 are the primary products. At high oxygen surface concentrations, CO and H2 cannot desorb without oxidation and then, CO_2 and H_2O are the main products.

In our work, the support seems to play an important role on determination of reaction mechanism. Apparently, this is not related to the redox properties of the support since Pt/Al_2O_3 also exhibited the indirect mechanism.

The temperature programmed reduction results helped to understand the difference between the several catalysts. Pt/Al_2O_3 showed a typical TPR profile corresponding to the formation of a PtO_xCl_y surface complex [10], while for Pt/CeO_2 the first peak is related to the simultaneous reduction of surface CeO_2 and of the platinum precursor, while the second peak is related to the reduction of bulk CeO_2 [23]. Additionally, our

temperature programmed reduction results were consistent to the formation of a compound between Pt and Y_2O_3 as Pt/Y_2O_3 presented an additional peak of reduction at 420 °C that may be tentatively ascribed to the reduction of a $PtYO_3$ surface compound.

Ruckenstein and Wang [24] found that depending on the calcinations temperature of the Rh/Y_2O_3 catalyst, there was the formation of a compound between Rh and Y_2O_3 ($RhYO_3$). The formation of this compound was related to a strong interaction between Rh and the support. Furthermore, when the $RhYO_3$ compound was formed, there was an increase in the stability of Rh/Y_2O_3 in the partial oxidation of methane at temperatures higher than 800 °C. This increase in stability was explained by the generation of a quasi-steady state concentration of metallic sites under reaction conditions, when the reaction was performed at temperatures at which strong interaction between the metal and the support could be induced.

Therefore, the working catalyst goes through a redox process due to the coexistence of reductive and oxidative reactants. For Pt/Al_2O_3, Pt/CeO_2 and Pt/ZrO_2 catalysts, the surface platinum atoms are initially partially oxidized leading to the formation of full oxidation products (CO_2 and H_2O), followed by steam and dry reforming. In the case of Pt/Y_2O_3 the interaction between Pt and Y_2O_3 caused a moderation in the rates of oxidation and reduction of the metal particle with the formation of a quasi-steady state concentration of metallic sites during reaction conditions. This would explain why the Pt/Y_2O_3 does not show the combustion route at lower temperatures as observed for the other catalysts. This way, in the case of Pt/Y_2O_3 there is a change in the mechanism of reaction, allowing the occurrence of a direct mechanism. A important influence of the presence of Y_2O_3 was also reported previously [25].

For coke-free clean conditions, Wei and Iglesia [26] demonstrated a kinetic mechanism equivalence between CO_2, H_2O reforming, and CH_4 decomposition. First, all these reactions would be limited by the C–H .activation on Pt crystallite surfaces and unaffected by the presence of the co-reactants. The variation of turnover rates was explained by a change in dispersion, but there was not any variation in turnover frequencies by the change in the support. However, we have run our experiments under more severe conditions so that the catalysts were more exposed to deactivation by carbon deposition. As seen in the results section, the presence of the Pt–Y_2O_3 interaction affects not only the reaction mechanism but also the catalyst stability. The literature has several evidences of the key role of the support on the stability of the catalysts on the partial oxidation of methane [2, 6, 16–18, 24]. We have previously reported that oxygen mobility on the support is important for establishing a cleaning mechanism of the metal surface, removing the coke formed during the reaction [9, 10, 23], and that effect is due to the high oxygen storage properties of CeO_2 and $CeO_2{\cdot}ZrO_2$ [27, 28].

In this work, the deactivation observed for Pt/Al_2O_3, Pt/ZrO_2, and Pt/CeO_2 ppt could be attributed to their low oxygen transfer capacity (Table 1), which led to the carbon deposit around or near the metal particle. The coke formation inhibited the CO_2 dissociation on CO_2 reforming of methane. This affects the second step of the indirected mechanism of the partial oxidation of methane, which comprehends the CO_2 and steam reforming of unreacted methane. The higher oxygen storage capacity of Pt/CeO_2 catalyst kept the metal surface clean and promoted the stability of the catalyst.

On the other hand, Pt/Y_2O_3 proved to be quite stable even though it has not presented any oxygen storage capacity. The interaction of platinum and yttria seemed to be responsible for the increase in the stability of the catalyst. The Ruckenstein and Wang [24] suggestion for Rh/Y_2O_3 catalysts of a formation of a quasi-steady-state concentration of metallic sites due to a moderation of the oxidation and reduction rates of the metal particles may be playing a role. Additionally, we may point out that the interaction between platinum and yttria may have led to a protection of the metal particles for carbon deposition by means of an ensemble effect as already established by Trimm [29], and by Rostrup-Nielsen [30] for methane conversion.

5. Conclusions

For Pt/Al_2O_3, Pt/ZrO_2 and Pt/CeO_2 catalysts, temperature programmed surface reaction (TPSR) analysis showed the partial oxidation of methane occurs in two steps: combustion of methane followed by H_2O and CO_2 reforming of unreacted methane, while for Pt/Y_2O_3 a direct mechanism was observed. Pt/CeO_2 catalysts showed the higher stability in the partial oxidation of methane. The results may be explained by the higher reducibility and capacity to store/release oxygen allowing a continuous cleaning of the actives sites from the carbon deposition. For the Pt/Al_2O_3, and Pt/ZrO_2 catalysts the increase in the carbon deposits close to the metal particles inhibit the CO_2 dissociation in the second step of CO_2 reforming of methane. Pt/Y_2O_3 catalyst was active in the partial oxidation of methane, and its stability may be explained by formation of a compound between Pt and yttria.

Acknowledgments

The authors acknowledge the financial support from CNPq, FINEP, FAPERJ and PETROBRAS.

References

[1] J.H. Lunsford, Catal. Today 63 (2000) 165.
[2] J.R. Rostrup-Nielsen and J. Sehested, Adv. Catal. 47 (2002) 65.
[3] S. Freni, G. Calogero and S. Cavallaro, J. Power Sources 87 (2000) 28.
[4] P.D.F. Vernon, M.L.H. Green, A.K. Cheetham and A.T. Ashcroft, Catal. Lett. 6 (1990) 181.
[5] P.M. Torniainen, X. Chu and L.D. Schmidt, J.Catal. 146 (1994) 1.
[6] Y. Boucouvalas, Z. Zhang and X.E. Verykios, Catal. Lett. 40 (1996) 189.
[7] A.A. Lemonidou, A.E. Stambouli, G.J. Tjatjopoulos and I.A. Vasalos, Catal. Lett. 43 (1997) 235.
[8] A.G. Steghuis, J.G. Van Ommen and J.A. Lercher, Catal. Today 46 (1998) 91.
[9] L.V. Mattos, E.R. de Oliveira, P.D. Resende, F.B. Noronha and F.B. Passos, Catal. Today 77 (2002) 245.
[10] L.V. Mattos, E. Rodino, D.E. Resasco, F.B. Passos and F.B. Noronha, Fuel Process. Technol. 1677 (2003) 1.
[11] C.E. Hori, H. Permana, K.Y.S. Ng, A. Brenner, K. More, K.M. Rahmoeller and D. Belton, Appl. Catal. Envir. B. 16 (1998) 105.
[12] F.B. Passos, M. Schmal and R. Frety, Catal. Lett. 14 (1992) 57.
[13] E. Rogemond, N. Essayem, R. Frety, V. Perrichon, M. Primet and F. Mathis, J. Catal. 166 (1997) 229.
[14] M. Pettre, Ch. Eichner and M. Perrin, Trans. Faraday Soc. 43 (1946) 335.
[15] D. Dissanayake, M.P. Rosynek, K.C.C. Kharas and J.H. Lunsford, J. Catal. 132 (1991) 117.
[16] M.E.S. Hegarty, A.M. O'Connor and J.R.H. Ross, Catal. Today 42 (1998) 225.
[17] M.M.V.M. Souza and M. Schmal, Appl. Catal. A: Gen. 281 (2005) 19.
[18] W.J.M. Vermeiren, E. Blomsma and P.A. Jacobs, Catal. Today 13 (1992) 421.
[19] E.P.J. Mallens, J.H.B.J. Hoebink and C.B. Marin, Catal. Lett. 33 (1995) 291.
[20] Y.H. Hu and E. Ruckenstein, J. Phys. Chem. A. 102 (1998) 10568.
[21] W.Z. Wheng, M.S. Chen, Q.G. Yan, T.H. Wu, Z.S. Chao, Y.Y. Liao and H.L. Wan, Catal. Today 63 (2000) 317.
[22] D. Wang, O. Dewaele, A.M. de Groote and G.F. Froment, J.Catal 159 (1996) 418.
[23] L.V. Mattos, E.R. Oliveira, P.D. Resende, F.B. Noronha and F.B. Passos, Catal. Today 101 (2005) 23.
[24] E. Ruckenstein and H. Wang, J. Catal. 190 (2000) 32.
[25] H. Nishimoto, K. Nakagawa, N. Ikenaga and T. Suzuki, Catal. Lett. 82 (2002) 161.
[26] J. Wei and E.J. Iglesia, J. Phys. Chem. B 108 (2004) 4094.
[27] M.H. Yao, R.J. Baird, F.W. Kunz and T.E. Hoost, J. Catal. 166 (1997) 67.
[28] J. Kaspar, P. Fornasiero and M. Graziani, Catal. Today 50 (1999) 285.
[29] D.L. Trimm, Catal. Today 49 (1999) 3.
[30] J.R. Rostrup- Nielsen and I. Alstrup, Catal. Today 53 (1999) 311.